Oxidation of methionine residues activates the high-threshold heat-sensitive ion channel TRPV2

Tabea C. Fricke[a], Frank Echtermeyer[a], Johannes Zielke[a], Jeanne de la Roche[b], Milos R. Filipovic[c,d], Stéphane Claverol[e], Christine Herzog[a], Makoto Tominaga[f], Ruth A. Pumroy[g], Vera Y. Moiseenkova-Bell[g], Peter M. Zygmunt[h], Andreas Leffler[a,1], and Mirjam J. Eberhardt[a]

[a]Department of Anesthesiology and Intensive Care Medicine, Hannover Medical School, 30625 Hannover, Germany; [b]Institute for Neurophysiology, Hannover Medical School, 30625 Hannover, Germany; [c]Institut de Biochimie et Génétique Cellulaires, Université de Bordeaux, UMR 5095, F-33077 Bordeaux, France; [d]CNRS, Institut de Biochimie et Génétique Cellulaires, Université de Bordeaux, UMR 5095, F-33077 Bordeaux, France; [e]Plateforme Protéome Centre Genomique Fonctionnelle Bordeaux, Université de Bordeaux, 33076 Bordeaux Cedex, France; [f]Division of Cell Signaling, Okazaki Institute for Integrative Bioscience, National Institute of Natural Sciences, 444-8787 Okazaki, Japan; [g]Department of Systems Pharmacology and Translational Therapeutics, Perelman School of Medicine, University of Pennsylvania, Philadelphia, PA 19104; and [h]Department of Clinical Sciences Malmö, Lund University, SE-205 02 Malmö, Sweden

Edited by Ramon Latorre, Centro Interdisciplinario de Neurociencias de Valparaíso, Facultad de Ciencias, Universidad de Valparaíso, Valparaíso, Chile, and approved October 4, 2019 (received for review March 21, 2019)

Thermosensitive transient receptor potential (TRP) ion channels detect changes in ambient temperature to regulate body temperature and temperature-dependent cellular activity. Rodent orthologs of TRP vanilloid 2 (TRPV2) are activated by nonphysiological heat exceeding 50 °C, and human TRPV2 is heat-insensitive. TRPV2 is required for phagocytic activity of macrophages which are rarely exposed to excessive heat, but what activates TRPV2 in vivo remains elusive. Here we describe the molecular mechanism of an oxidation-induced temperature-dependent gating of TRPV2. While high concentrations of H_2O_2 induce a modest sensitization of heat-induced inward currents, the oxidant chloramine-T (ChT), ultraviolet A light, and photosensitizing agents producing reactive oxygen species (ROS) activate and sensitize TRPV2. This oxidation-induced activation also occurs in excised inside-out membrane patches, indicating a direct effect on TRPV2. The reducing agent dithiothreitol (DTT) in combination with methionine sulfoxide reductase partially reverses ChT-induced sensitization, and the substitution of the methionine (M) residues M528 and M607 to isoleucine almost abolishes oxidation-induced gating of rat TRPV2. Mass spectrometry on purified rat TRPV2 protein confirms oxidation of these residues. Finally, macrophages generate TRPV2-like heat-induced inward currents upon oxidation and exhibit reduced phagocytosis when exposed to the TRP channel inhibitor ruthenium red (RR) or to DTT. In summary, our data reveal a methionine-dependent redox sensitivity of TRPV2 which may be an important endogenous mechanism for regulation of TRPV2 activity and account for its pivotal role for phagocytosis in macrophages.

TRPV2 | redox sensitivity | methionine | oxidation | phagocytosis

Transient receptor potential (TRP) ion channels enable organisms to regulate body temperature and to detect and react to changes in ambient temperature. Thermosensitive sensory neurons are equipped with a subset of TRP channels exhibiting different temperature thresholds (1–3), and a recent study identified TRP vanilloid (TRPV) TRPV1, TRPA1, and TRPM3 as redundant heat sensors allowing a fault-tolerant detection of painful heat (4). A role as heat receptor was also suggested for TRPV2 which is activated by temperatures exceeding 50 °C (5). TRPV2 is predominantly expressed in myelinated neurons and was postulated to account for the high threshold of type 1 mechanosensitive and heat-sensitive Aδ-fibers which have been described in rodents and humans (5–7). However, mice lacking TRPV2 display an intact heat sensitivity (8), and human TRPV2 is even heat-insensitive (9). Thus, the relevance of the heat sensitivity of TRPV2 observed in vitro remains elusive (10). TRPV2 is also expressed in nonneuronal tissues, including macrophages which require TRPV2 for phagocytosis (11). A similar role in macrophages was described for TRP melastatin 2 (TRPM2), which also regulates body temperature and accounts for sensation of warmth (12–16). Kashio et al. (12) suggested that intracellular reactive oxygen species (ROS) in macrophages activate TRPM2 and showed that H_2O_2-induced sensitization of TRPM2 is due to oxidation of an N-terminal methionine residue. The redox sensitivities of other TRP channels like TRP ankyrin (TRPA) TRPA1 and TRPV1, however, depend on N-terminal cysteine residues (17–19). Considering the overlapping roles for TRPV2 and TRPM2 in macrophages and that several TRP channels are modified by oxidation, we explored the redox sensitivity of TRPV2.

Results

Oxidation Sensitizes and Activates Rodent and Human TRPV2. Rat TRPV2 (rTRPV2) transiently expressed in HEK 293t cells was examined with the whole-cell patch clamp technique. As was previously described (5, 20, 21), heated external solution (~50 °C) evoked inward currents displaying decreasing temperature thresholds and increasing amplitudes upon repetitive activation (*SI Appendix*, Fig. S1*A*; $n = 7$). In contrast, repeated applications of heat around 45 °C failed to evoke inward currents (*SI Appendix*, Fig. S1*B*; $n = 7$). Heat-evoked inward currents could also be

Significance

Redox sensitivity is a common property of temperature-sensitive transient receptor potential (TRP) ion channels. Here we show that oxidation sensitizes and activates rodent TRPV2 orthologs known to have a high temperature threshold (>50 °C), but also the heat-insensitive human TRPV2. This oxidation-induced channel gating is intact in cell-free membrane patches, cysteine-independent but reduced upon replacement of the methionine residues M528 and M607. Blocking of TRPV2 and the reducing agent DTT reduce phagocytosis in macrophages which also generate heat-induced membrane currents following oxidation. These data reveal a methionine-dependent redox sensitivity of TRPV2 which may resemble a decisive endogenous mechanism enabling channel activation.

Author contributions: F.E., J.d.l.R., M.R.F., C.H., A.L., and M.J.E. designed research; T.C.F., F.E., J.Z., J.d.l.R., M.R.F., S.C., R.A.P., A.L., and M.J.E. performed research; M.T., R.A.P., V.Y.M.-B., and P.M.Z. contributed new reagents/analytic tools; T.C.F., F.E., J.Z., J.d.l.R., M.R.F., C.H., V.Y.M.-B., A.L., and M.J.E. analyzed data; and T.C.F., P.M.Z., A.L., and M.J.E. wrote the paper.

The authors declare no competing interest.

This article is a PNAS Direct Submission.

[1]To whom correspondence may be addressed. Email: leffler.andreas@mh-hannover.de.

This article contains supporting information online at www.pnas.org/lookup/suppl/doi:10.1073/pnas.1904332116/-/DCSupplemental.

First published November 12, 2019.

evoked in cells expressing mouse TRPV2 (mTRPV2; *SI Appendix*, Fig. S1*C*), but not human TRPV2 (hTRPV2; *SI Appendix*, Fig. S1*D*; $n = 6$) which was previously shown to be heat-insensitive (9). As the threshold around 50 °C found for rTRPV2 was considerably lower than the ∼55 °C that was previously reported (20), we compared the experimental conditions in both studies. While we used sodium hydroxide (NaOH) to adjust the pH value in the extracellular solution, tetramethylammonium hydroxide (TMA-OH) was used in the previous study (20). Quaternary ammonium cations inhibit TRPV2 (22), and, with an extracellular solution buffered with TMA-OH, we found that the threshold for activation of rTRPV2 increased to 57 ± 1 °C (*SI Appendix*, Fig. S1 *E* and *F*). We proceeded with NaOH-based solutions in this study.

While micromolar concentrations of H_2O_2 gate TRPV1 and TRPM2 (12, 19, 23), rTRPV2 required 10 mM H_2O_2 applied for >20 min to generate small heat-evoked currents which were blocked by ruthenium red (RR; Fig. 1*A*; $n = 5$). In contrast, the oxidant chloramine-T (ChT) induced a strong sensitization of rTRPV2 within 2 to 3 min (Fig. 1*B*). Heat-evoked inward currents increased from 16 ± 11 pA/pF to 487 ± 95 pA/pF following application of 1 mM ChT ($n = 14$, $P < 0.001$; Fig. 1*C*). The threshold for activation dropped from 50 ± 0.7 °C to 37 ± 1 °C ($P < 0.001$, Wilcoxon matched pair test), and the effect of ChT was concentration-dependent (Fig. 1*D*). Similar ChT-induced effects were observed in cells expressing mTRPV2 (*SI Appendix*, Fig. S1*G*), as well as hTRPV2 ($n = 7$; Fig. 1*E*). As the effect of ChT on TRPV2 was irreversible

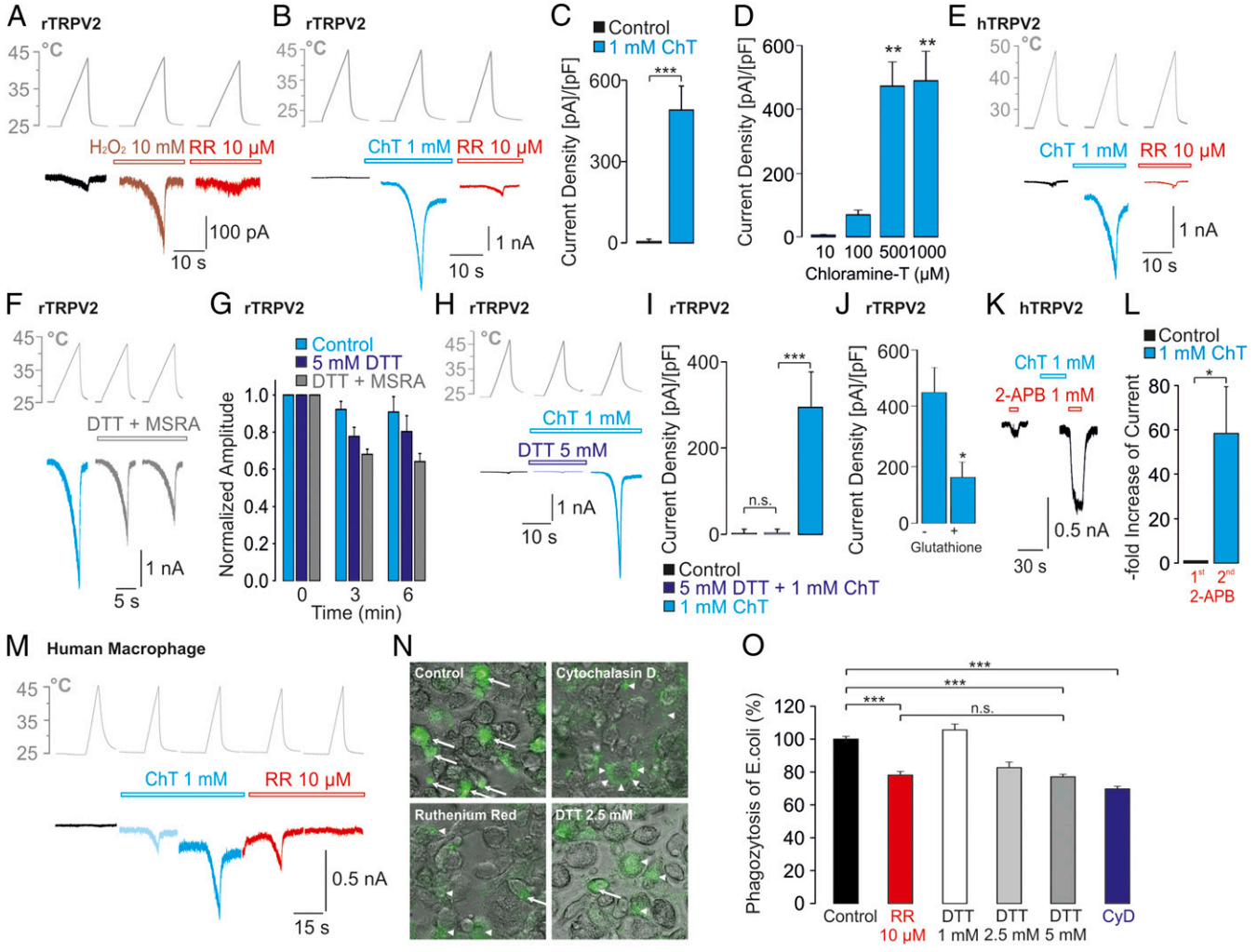

Fig. 1. H_2O_2 and ChT sensitize TRPV2. (*A*) Ten millimolars H_2O_2 applied for >20 min ($n = 5$) and (*B*) 1 mM ChT applied for 3 to 4 min ($n = 14$) induce heat-evoked currents which are blocked by RR. (*C*) Bar diagram of mean current densities of heat-evoked currents following 1 mM ChT ($P < 0.001$). (*D*) ChT sensitizes rTRPV2 in a concentration-dependent manner. Bars display the current density of heat-evoked currents ($n = 5$ to 14, ANOVA $F[3, 37] = 10.314$, $P < 0.001$; followed by HSD post hoc test, $P < 0.01$). (*E*) One millimolar ChT induces heat sensitivity of hTRPV2. (*F*) Induction of rTRPV2-mediated heat-evoked currents by ChT is partially reversed by DTT and MSRA. (*G*) Bar diagram of mean current densities of 3 heat-evoked currents induced by 1 mM ChT. DTT was applied after the first current, and MSRA was included in the pipette solution ($n = 6$ to 8). (*H* and *I*) Mean current densities of rTRPV2-mediated heat-evoked currents do not increase following application of ChT combined with DTT ($P = 0.97$), but by application of ChT alone ($P < 0.001$, $n = 9$, ANOVA $P < 0.001$, followed by HSD post hoc test). (*J*) ChT-induced heat-evoked currents are reduced by 10 mM glutathione in the pipette solution ($P < 0.05$, $n = 8$, Mann–Whitney *U* test). (*K* and *L*) One millimolar ChT applied for 3 min sensitizes currents induced by 1 mM 2-APB ($n = 8$, $P < 0.05$, Wilcoxon matched pairs test). (*M*) Human macrophages produce ChT-induced heat-evoked currents blocked by RR ($n = 7$). (*N*) Images of macrophages with fluorescent signals for fluorescein isothiocyanate-labeled *E. coli* display a strong fluorescent signal in the cytosol, demonstrating phagocytosis under control settings. Inhibition of phagocytosis was examined for cytochalasin D, RR, and DTT. (*O*) Bar graph displaying the effectivity of macrophages to phagocyte *E. coli*. The addition of 10 μM RR as well as DTT reduced phagocytosis. Cytochalasin D (CyD) prevents actin polymerization and was applied as a control. Kruskal–Wallis test followed by Dunn's multiple comparison test. Data are given as mean ± SEM. *$P < 0.05$; **$P < 0.01$; ***$P < 0.001$; and n.s., not significant.

following washout, we next examined whether it can be chemically reversed. While dithiothreitol (DTT) is effective to reduce cysteine oxidation, it lacks effect on methionine sulfoxide [Met(O)] which can only be enzymatically reduced by methionine sulfoxide reductase (MSRA) (24, 25). In the presence of DTT, MSRA can convert Met(O) to methionine in vitro (24, 25). While extracellular application of 5 mM DTT following ChT treatment resulted in a partial but nonsignificant reversal of heat-evoked currents, we observed a significant reversal when MSRA (10 μg/mL) was included in the pipette solution (Fig. 1 *F* and *G*, $n = 6$ to 8 in each group; $P < 0.002$ ANOVA honestly significant difference [HSD] post hoc test). Indicating that DTT can scavenge or neutralize oxidants, ChT failed to sensitize rTRPV2 when applied together with 5 mM DTT ($n = 9$; Fig. 1 *H* and *I*). Furthermore, 10 mM glutathione included in the pipette solution reduced ChT-induced heat-evoked currents (Fig. 1*J*; $n = 8$, $P < 0.05$, Mann–Whitney *U* test). The ability of ChT to remove fast inactivation of voltage-gated sodium currents is due to oxidation of methionine residues, a property which is lost following storage of ChT at room temperature (26, 27). When we explored the effect of ChT stored at room temperature for >24 h, this "inactivated" ChT (1 mM) failed to induce a sensitization of rTRPV2 (*SI Appendix*, Fig. S1 *H* and *I*). ChT also induced a potentiation of inward currents induced by 200 μM 2-aminoethoxydiphenylborate (2-APB) on rTRPV2 (*SI Appendix*, Fig. S1 *J* and *K*). Although hTRPV2 was reported to be 2-APB–insensitive (22), hTRPV2-mediated inward currents evoked by 1 mM 2-APB were potentiated by 1 mM ChT ($n = 8$, $P < 0.02$; Fig. 1 *K* and *L*).

TRPV2 is functionally expressed in the cell membrane of human and mouse macrophages (5, 28), and thus we asked whether macrophages produce heat-evoked inward currents following oxidation. Indeed, both mouse (*SI Appendix*, Fig. S2*A*) and human ($n = 7$; Fig. 1*M*) macrophages treated with 1 mM ChT generated small inward currents which were potentiated by heat and inhibited by RR. In agreement with the poor efficacy of H_2O_2 on recombinant rTRPV2, 10 mM H_2O_2 failed to induce heat-evoked inward currents in macrophages which did not allow stable recordings for >20 min (*SI Appendix*, Fig. S2 *B* and *C*). We also explored whether blocking of TRPV2 by RR or inhibition of oxidation by DTT reduces phagocytosis of fluorescent *Escherichia coli* bioparticles (Fig. 1*N*). Indeed, 10 μM RR reduced phagocytosis by 22 ± 2% ($n = 38$; Fig. 1*O*). DTT also reduced phagocytosis in a concentration-dependent manner with a reduction of 23 ± 2% by 5 mM DTT ($n = 15$; Fig. 1*O*). While our data suggest that ChT sensitizes TRPV2, experiments on both HEK 293t cells with TRPV2 and macrophages also revealed small ChT-induced inward currents at room temperature. These currents were blocked by RR and thus do not seem to result from nonspecific leak currents. When monitored during 500-ms-long voltage ramps ranging from −100 mV to 100 mV, these currents exhibited an outward rectification for both rTRPV2 (Fig. 2*A*) and hTRPV2 (*SI Appendix*, Fig. S2*D*). We hypothesized that these ChT-evoked responses result from a direct activation of TRPV2 due to lowering its temperature threshold below room temperature. To test this hypothesis, 1 mM ChT was applied for 3 min on cells held at −60 mV at either room temperature or 37 °C. ChT induced inward currents which were blocked by RR in rTRPV2-expressing cells (Fig. 2*B*; $n = 6$), but not in nontransfected HEK 293t cells (Fig. 2*C*; $n = 7$). When examined at 37 °C, ChT induced significantly larger TRPV2-mediated inward currents (Fig. 2 *B* and *D*; $n = 5$, $P < 0.05$, Mann–Whitney *U* test). Similar effects were observed for cells expressing hTRPV2 (*SI Appendix*, Fig. S2 *E* and *F*). This direct ChT-induced activation of TRPV2 also became evident in calcium imaging experiments conducted at temperatures of >30 °C (Fig. 2 *E* and *F* and *SI Appendix*, Fig. S3 *A–E*). In order to substantiate these data and to examine whether ChT oxidizes the TRPV2 protein itself or rather cytosolic proteins interacting with TRPV2, we performed single-channel recordings on cell-free inside-out patches at 30 °C. As demonstrated in Fig. 2 *G–J*, a gradually increasing activation of channel openings induced by 500 μM ChT was inhibited by RR ($n = 6$). ChT also potentiated 2-APB–induced channel openings in inside-out patches (*SI Appendix*, Fig. S3 *F–J*). These data indicate that gating of TRPV2 by ChT is due to an oxidation of TRPV2.

As H_2O_2 seems to only marginally sensitize TRPV2, we next explored the effects of further oxidants on TRPV2. The cysteine-selective oxidants methanethiosulfonate ethylammonium (MTSEA) (*SI Appendix*, Fig. S4*A*) and diamide were ineffective on TRPV2 (*SI Appendix*, Fig. S4*B*). Chuang and Lin (19) demonstrated that the cysteine-dependent H_2O_2-induced sensitization of TRPV1 is inhibited by a substance which covalently binds to and occupies cysteines. The TRPA1 agonist allyl isothiocyanate (AITC)—known to covalently bind to cysteines—indeed prevented sensitization of heat-evoked inward currents on hTRPV1 by 10 mM H_2O_2 (*SI Appendix*, Fig. S4 *C* and *D*). In contrast, treatment of rTRPV2-expressing cells with AITC did not prevent ChT-induced sensitization of heat-evoked inward currents (*SI Appendix*, Fig. S4 *E* and *F*). Furthermore, the methionine-preferring oxidant *N*-chlorosuccinimide sensitized both rTRPV2 (Fig. 2 *K* and *L*; $P < 0.05$, $n = 8$) and hTRPV2 (*SI Appendix*, Fig. S4*G*). As was previously demonstrated for TRPA1 (29, 30), exposure to ultraviolet A (UVA) light for 3 to 4 min induced heat-evoked inward currents in cells expressing rTRPV2 (Fig. 2 *M* and *N*; $P < 0.01$, $n = 12$), but also mTRPV2 and hTRPV2 (*SI Appendix*, Fig. S4 *H* and *I*). UVA light also evoked outwardly rectifying membrane currents elicited by voltage ramps (*SI Appendix*, Fig. S4*J*), and a potentiation of inward currents evoked by 2-APB (*SI Appendix*, Fig. S4 *K* and *L*). UVA light triggers the production of intracellular ROS such as singlet oxygen ($^1O_2$), hydroxyl radicals (OH·), and superoxide anions (O_2·−). However, neither tert-butyl-hydroperoxide nor the singlet oxygen donor Rose Bengal sensitized rTRPV2 (*SI Appendix*, Fig. S4 *M* and *N*). We adopted a strategy from Takeuchi and Yoshii (31) demonstrating that illumination of the fluorescent dye Lucifer Yellow (LY) included in the patch pipette triggers production of superoxide anions. When LY (500 μM) was applied through the patch pipette and illuminated, rTRPV2-expressing cells produced heat-evoked currents ($P < 0.05$, $n = 8$; Fig. 2 *O* and *P*) as well as ramp currents at room temperature (*SI Appendix*, Fig. S4*O*). LY-induced effects were also observed on hTRPV2 (*SI Appendix*, Fig. S4*P*). Similar photosensitizing effects were previously demonstrated for streptozotocin (STZ) on TRPA1 (32), and for protoporphyrine IX (PPIX) on TRPA1 and TRPV1 (30). When applied in combination with UVA light through the green fluorescent protein filter insufficient to evoke effects by itself, STZ (100 μM; Fig. 2 *Q* and *R*; $n = 8$, $P < 0.01$) and PPIX (1 μM; Fig. 2 *S* and *T*; $n = 7$, $P < 0.05$) induced heat-evoked inward currents which were blocked by RR. As is exemplified for PPIX in Fig. 2*U*, photosensitizers also evoked rTRPV2-mediated currents at room temperature.

Oxidation-Induced Sensitization of rTRPV2 Depends on Methionine Residues. Our interpretation of the data collected to this point is that oxidants, including intracellular ROS, oxidize methionine rather than cysteine residues to gate TRPV2. When aligning the sequences of rTRPV2 and hTRPV2, we identified 11 conserved methionine residues. Site-directed mutagenesis was performed to introduce single alanine substitutions for all of these methionine residues. While 7 mutants exhibited robust heat-evoked inward currents following application of 1 mM ChT, ChT failed to induce heat-evoked currents in 4 constructs (M528A, M607A, M640A, and M645A; *SI Appendix*, Fig. S5*A*; $n = 4$ to 14 for each construct). While rTRPV2-M607A generated 2-APB–induced inward currents and was thus functional, no currents were observed in cells expressing the nonfunctional constructs rTRPV2-M528A, rTRPV2-M640A, and rTRPV2-M645A (*SI Appendix*, Fig. S5*A*). When performing more-conservative substitutions

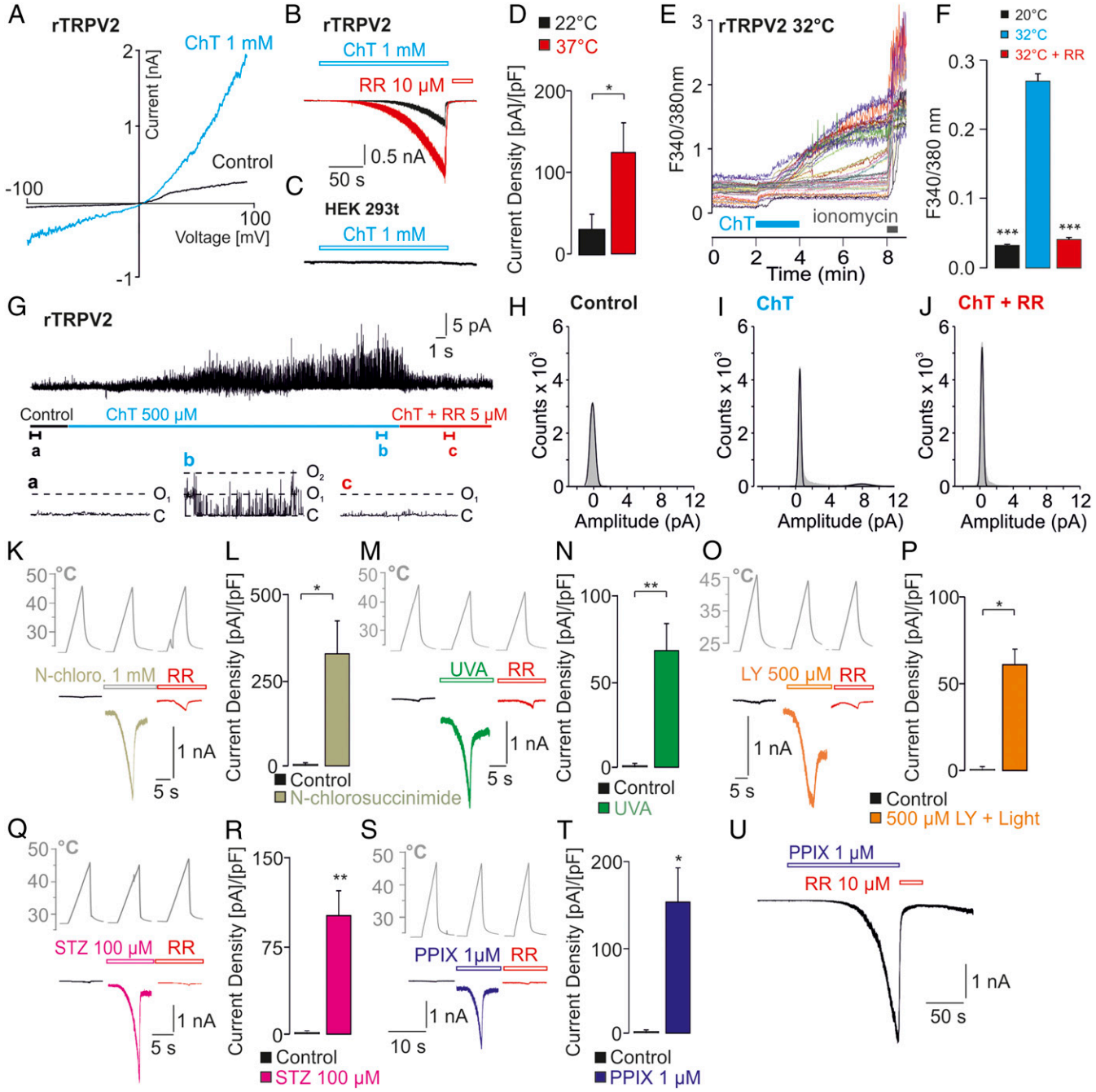

Fig. 2. Oxidation activates TRPV2. (*A*) Outwardly rectifying membrane currents monitored during 500-ms-long voltage ramps from −100 mV to 100 mV before and after 1 mM ChT. (*B*) Inward current induced by 1 mM ChT applied for 3 min on cells held at −60 mV. Experiments were performed at room temperature (black trace, $n = 5$) or at 37 °C (red trace, $n = 5$). (*C*) ChT does not induce currents in nontransfected HEK 293t cells ($n = 5$). (*D*) Bar diagram of mean current densities of ChT-induced inward currents at room temperature and 37 °C ($n = 5$ and 6, $P < 0.05$, Mann–Whitney *U* test). (*E*) Calcium imaging on rTRPV2-transfected cells performed at 32 °C; 400 µM ChT induced an increase in intracellular calcium. Note that traces with different colors represent individual cells. (*F*) Bar diagrams of increase in intracellular calcium (ANOVA $F[2, 2{,}028] = 440.29$, $P < 0.001$; followed by HSD post hoc test $^*P < 0.001$). (*G*) Single-channel recordings on rTRPV2 performed on inside-out patches held at +60 mV at 30 °C. Channel openings induced by 500 µM ChT are inhibited by RR. Sections a, b, and c represent episodes of 1 s of the upper trace. (*H–J*) Amplitude histograms calculated from 5-s sections of the full trace. (*K–T*) Recordings on rTRPV2-HEK 293t cells exposed to heat before and during application of (*K* and *L*) 1 mM *N*-chlorosuccinimide ($n = 9$, $P < 0.05$), (*M* and *N*) UVA light ($n = 12$, $P < 0.01$), (*O* and *P*) LY (500 µM) in the patch pipette together with light ($n = 8$, $P < 0.05$), (*Q* and *R*) STZ (100 µM, $n = 8$, $P < 0.01$) and (*S* and *T*) PPIX (1 µM, $n = 8$, $P < 0.05$) applied together with UVA light (Wilcoxon matched pairs test). (*U*) PPIX applied together with UVA light activates rTRPV2. Data are given as mean ± SEM. $^*P < 0.05$; $^{**}P < 0.01$; $^{***}P < 0.001$.

with isoleucine at these positions, the substitutions M640I and M645I again resulted in nonfunctional channels. However, replacement of M528 or M607 with isoleucine resulted in functional channels which generated ChT-induced heat-evoked currents with significantly reduced amplitudes compared to wild-type rTRPV2 (rTRPV2-WT) (Fig. 3 *A*, *B*, and *D*; $n = 8$–14 ANOVA $F[3, 36] = 14.309$, $P < 0.001$, ANOVA HSD post hoc test). In the double-mutant rTRPV2-M528I/M607I, ChT almost completely failed to

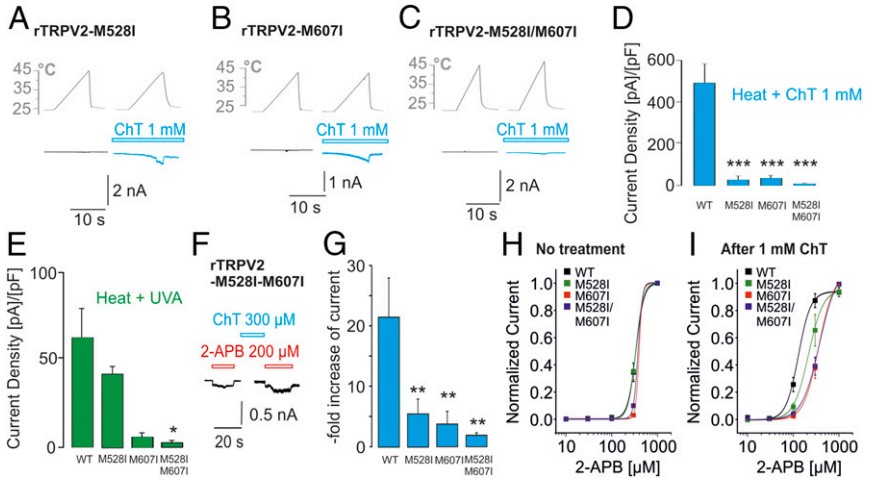

Fig. 3. Methionine residues dictate oxidation-induced sensitization of TRPV2. (*A*–*C*) Traces of (*A*) rTRPV2-M528I ($n = 8$), (*B*) rTRPV2-M607I ($n = 8$), and (*C*) rTRPV2-M528I/M607I ($n = 10$) evoked by heat induced by 1 mM ChT. (*D* and *E*) Bar diagrams of mean current densities of currents induced by ChT (*D*) or UVA light (*E*) ($n = 4$–14 each). (*F*) Traces of rTRPV2-M528I/M607I displaying the effect of 300 µM ChT on inward currents induced by 200 µM 2-APB. ChT was applied for 3 min ($n = 10$). (*G*) Average potentiation of 2-APB–induced inward currents by ChT on rTRPV2-WT, rTRPV2-M528I, rTRPV2-M607I, and rTRPV2-M528I/M607I. Data were normalized ($n = 7$ to 10). (*H* and *I*) Dose–response curves for 2-APB–evoked inward currents of rTRPV2-WT and mutant constructs (*H*) without treatment and (*I*) after 1 mM ChT. Normalized data were plotted against the corresponding concentrations of 2-APB and fitted with the Hill equation ($n = 6$ to 8 for each concentration). Data are given as mean ± SEM. $*P < 0.05$; $**P < 0.01$; $***P < 0.001$; n.s., not significant.

induce heat-evoked currents (Fig. 3 *C* and *D*; $n = 10$). When challenged with UVA light, rTRPV2-M528I/607I generated only marginal heat-induced inward currents (Fig. 3*E*; $n = 4$ to 12 for each construct, $P < 0.05$, ANOVA). The sensitizing effect of 1 mM ChT on 2-APB–induced currents was also significantly reduced in all 3 mutants (Fig. 3 *F* and *G*; $n = 7$ to 10). All 3 mutant constructs appear to be functional, as they produce high-threshold heat-evoked currents (*SI Appendix*, Fig. S5 *B–D*), and displayed similar concentration dependencies for 2-APB–evoked activation as rTRPV2-WT (Fig. 3*H* and *SI Appendix*, Fig. S5*E*; $n = 6$ to 8 for each mutant). Following treatment with 1 mM ChT, however, the leftward shift of the dose–response curve was more pronounced for rTRPV2-WT than for the mutants (Fig. 3*I* and *SI Appendix*, Fig. S5*E*). These data suggest that, while replacement of M528 and M607 does not severely impair the functionality of rTRPV2, it removes oxidation-induced gating.

For identification of a ChT-induced oxidation of methionine, we exposed 0.1 mM methionine to 1 mM ChT for 15 min at 37 °C and observed an $m/z = 16$ rightward shift in mass spectrum, demonstrating a methionine oxidation (*SI Appendix*, Fig. S5*F*). We next treated purified rTRPV2 protein with ChT or H_2O_2 (10-fold excess) for 15 min at 37 °C. The proteins were then desalted and subjected to trypsin digestion. Comparison of tandem mass spectrometry analysis of tryptic digests of samples treated with oxidants and untreated samples indeed confirmed that M528 (ChT 28%; H_2O_2 16%; *SI Appendix*, Fig. S6) and M607 (ChT 4%; H_2O_2 22%; *SI Appendix*, Fig. S7) are the most heavily oxidized methionine residues in TRPV2. Mass spectrometry data also identified M671 (ChT 13%; H_2O_2 12%; *SI Appendix*, Fig. S8) and, to a lesser extent, M372 (ChT 0.4%; H_2O_2 0%; *SI Appendix*, Fig. S9) as further possible target residues for oxidation-induced activation. However, we found that replacement of M671 with isoleucine (rTRPV2-M671I) did not reduce ChT-induced heat-evoked inward currents (*SI Appendix*, Fig. S5 *G* and *I*). Furthermore, the double-mutant rTRPV2-M528I/M671I did not generate smaller heat-evoked currents following ChT treatment as compared to rTRPV2-M528I (*SI Appendix*, Fig. S5 *H* and *I*).

The Heat Sensors TRPM2 and TRPV1 Discriminate between Oxidants. The data from the purified TRPV2 protein did not explain the poor efficacy of H_2O_2 which sensitizes the heat-sensitive TRP channels TRPM2 and TRPV1 (12, 19). H_2O_2-induced sensitization of hTRPM2 depends on a single methionine residue (M215) (12), and we asked whether M215 accounts for sensitivity to ChT and UVA light. While the hTRPM2-M215A mutant is H_2O_2-insensitive (*SI Appendix*, Fig. S10 *A* and *B*), even hTRPM2-WT was not sensitized by UVA light (*SI Appendix*, Fig. S10*C*). One millimolar ChT induced a sensitization of both hTRPM2-WT and hTRPM2-M215A, although the current densities were significantly smaller in the mutant (*SI Appendix*, Fig. S10 *D–F*). TRPV1 was reported to be regulated by a cysteine-dependent redox regulation (19). We explored whether H_2O_2, ChT, and UVA light induce differential effects on TRPV1 as well. H_2O_2-induced (10 mM) sensitization of hTRPV1-mediated heat-evoked inward currents was abolished following substitutions of C158, C391, and C767 (hTRPV1-3C; *SI Appendix*, Fig. S10 *G* and *H*). Supporting a previous study (23), 1 mM ChT only induced a minor sensitization of hTRPV1-WT (*SI Appendix*, Fig. S10*I*). UVA light strongly sensitized heat-evoked inward currents generated by both hTRPV1-WT ($n = 12$; *SI Appendix*, Fig. S10*J*) and the hTRPV1-3C mutant ($n = 8$; *SI Appendix*, Fig. S10 *K* and *L*). These data demonstrate that not only TRPV2 discriminates among oxidants in a not fully predictable manner.

Discussion

In the present study, we describe a yet unrecognized redox sensitivity of TRPV2. Rodent orthologs of TRPV2 are activated by nonphysiological temperatures exceeding 50 °C (5, 20), and our data show that oxidation reduces the temperature threshold for activation to body temperature or even lower. Oxidation also activates and sensitizes the heat-insensitive hTRPV2 (9). The redox sensitivity of TRPV2 was evident in intact cells as well as in cell-free membrane patches, indicating that channel gating results from an oxidation of the TRPV2 protein. Several experiments suggest that oxidation of methionine rather than cysteine residues accounts for TRPV2 channel activation. We also show that TRPV2, TRPV1, and TRPM2 discriminate between different

oxidants in a way which is not explained by mechanisms regarded to mediate redox sensitivity in these channels.

While several roles of TRPV2 for proper organ or cellular function have been described (11, 33–36), biophysical studies on TRPV2 are scarce. The lack of selective TRPV2 agonists as well as the high heat threshold for activation hamper detailed in vitro analyses. This notion particularly applies for hTRPV2, which is insensitive to both heat and 2-APB (9, 22). We demonstrate that the low 2-APB sensitivity of hTRPV2 is sensitized by oxidation, and that oxidation-induced activation is potentiated by heat. With no initial temperature threshold of hTRPV2, a shift in heat sensitivity can obviously not be determined. A genuine heat sensitivity may be predicted by temperature coefficients (Q_{10}) of >5 (37, 38). Q_{10} values for heat-induced potentiation of hTRPV2-mediated currents induced by ChT and *N*-chlorosuccinimide were calculated to be 2 ± 0.2 and 2.7 ± 0.3, respectively. Therefore, instead of postulating that oxidation renders hTRPV2 heat-sensitive, it seems more likely that high temperatures increase channel activity independent of a specific mechanism. Nevertheless, our data identify ROS as endogenous modulators of TRPV2 which, at body temperature, may even act as direct TRPV2 agonists. Redox sensitivity is a common property of temperature-sensitive TRP channels, but previous studies also examining TRPV2 did not detect this redox sensitivity (39). The poor efficacy of H_2O_2 and the complete lack of effects of cysteine-specific oxidants in TRPV2 is probably the main reason why this property has not yet been identified. As H_2O_2 oxidizes both cysteine and methionine, we do not have a clear explanation for this discrimination of TRPV2 between H_2O_2 and ChT. The limited duration of patch clamp recordings with application of aggressive oxidants complicates detection of what seem to be slow H_2O_2-induced effects on TRPV2. This notion is supported by our mass spectrometry data, suggesting that ChT and H_2O_2 oxidize essentially the same methionine residues, for example, M528 and M607. Thus, H_2O_2 might very well act as a relevant activator or sensitizer of TRPV2 in vivo. Of note is that a previous study from Tang and colleagues showed that modulation of calcium-activated potassium channels due to oxidation of methionine residues also discriminate between ChT and H_2O_2 when examined in vitro (25). Furthermore, our data on hTRPV1 and hTRPM2 demonstrate that they also discriminate between oxidants that, in theory, should induce similar effects. The previously reported redox-insensitive mutant constructs of TRPV1 (TRPV1-3C) and TRPM2 (hTRPM2-M215A) only demonstrate an abolished sensitivity to H_2O_2, but not to ChT (hTRPM2) and UVA light (hTRPV1). These data are intriguing and may suggest that all 3 TRP channels discriminate between distinct oxidants, allowing them to detect ROS in a partly redundant manner. Indeed, Chuang and Lin (19) discussed a similar discrimination of ROS detection between TRPA1 and TRPV1. Similar to the remaining redox sensitivities observed for hTRPV1-3C and hTRPM2-M215A, it seems likely that the redox sensitivity of TRPV2 per se does not only depend on M528I and M607. The characterization of rTRPV2 mutants requires a critical differentiation between a loss of redox sensitivity and loss of channel function, and although all mutants responded to high heat and 2-APB, our conclusions are subject to obvious limitations. In particular, it was impossible to examine the contributions of M640 and M645 for redox sensitivity, as these mutants were nonfunctional. While M640 and M645 are located within the lower gate in the channel pore, M607 forms the constriction site referred to as the upper gate (refs. 40 and 41 and *SI Appendix*, Fig. S11). It is likely that any conformational change induced by oxidation of these critical residues, including M528, can result in an altered functionality. Given that M528, M607, M640, and M645 are conserved in TRPV1, our findings may give rise to further functional and structural studies on these residues.

When referring to the physiological importance of the redox sensitivity of TRPV2, we found that H_2O_2, UVA light, and intracellular ROS can gate TRPV2. Sensitivity to UVA light may be relevant in the skin, where TRPV2 is expressed in sensory nerve endings, keratinocytes, and immune cells (42). ROS accumulate during hypoxia and ischemia, but are also downstream signaling molecules of membrane-bound receptors such as the toll-like receptor 4 coupling to NADPH oxidases (43). Kashio et al. (12) suggested that redox sensitivity of TRPM2 accounts for its crucial role in macrophages, allowing activation of TRPM2 by ROS in phagosomes. We found that inhibition of TRPV2 by RR (which does not block TRPM2) and the prevention of an oxidation by DTT results in reduced phagocytosis. Thus, similar to TRPM2, the redox sensitivity of TRPV2 may account for its role in macrophages where it is also located in phagosomes (16). The coexpression of TRPM2 and TRPV2 in macrophages may allow for a fault-tolerant ROS-induced signaling, or reflect specialized and nonoverlapping roles resulting from distinct abilities to detect ROS. While this and further redox-dependent properties of TRPV2 need to be substantiated in subsequent studies, our study identifies oxidation as a likely endogenous modulator of TRPV2.

Materials and Methods

A detailed description of the materials and methods is provided in *SI Appendix, SI Materials and Methods*.

Cell Culture. HEK 293t cells were transfected with different plasmids using jetPEI (Polyplus-transfection SA) as was described previously (44).

Human Peripheral Blood-Derived Macrophages. Macrophages were isolated from peripheral ethylenediaminetetraacete blood of volunteers by density gradient (Biocoll Separation Solution; Biochrom). Blood samples were collected by a staff anesthesiologist not involved in the project, and experimenters did not know the identity of the donors. Samples were anonymized and used only for isolation of macrophages.

Patch Clamp. Using an EPC10 USB HEKA amplifier (HEKA Electronik), whole-cell voltage clamp was performed on HEK 293t cells expressing hTRPV2, rTRPV2, mTRPV2, hTRPM2, or hTRPV1 and on macrophages.

Data Availability. MS data and cDNA mutant constructs are available upon request.

ACKNOWLEDGMENTS. We thank Kerstin Reher, Marina Golombek, and Heike Bürger (Department of Anesthesiology, Hannover Medical School) for technical assistance. The study was supported by the Department of Experimental Anesthesiology, Hannover Medical School. P.M.Z. was supported by the Swedish Research Council (Grant 2014-3801) and the Medical Faculty at Lund University. This work was supported by grants from the National Institute of Health (Grants R01GM103899 and R01GM129357 to V.Y.M.-B.). We thank Dr. Martin Fischer (Department of Neurophysiology, Hannover) for continuous support.

1. A. I. Basbaum, D. M. Bautista, G. Scherrer, D. Julius, Cellular and molecular mechanisms of pain. *Cell* **139**, 267–284 (2009).
2. A. Dhaka, V. Viswanath, A. Patapoutian, TRP ion channels and temperature sensation. *Annu. Rev. Neurosci.* **29**, 135–161 (2006).
3. J. Huang, X. Zhang, P. A. McNaughton, Modulation of temperature-sensitive TRP channels. *Semin. Cell Dev. Biol.* **17**, 638–645 (2006).
4. I. Vandewauw *et al.*, A TRP channel trio mediates acute noxious heat sensing. *Nature* **555**, 662–666 (2018).
5. M. J. Caterina, T. A. Rosen, M. Tominaga, A. J. Brake, D. Julius, A capsaicin-receptor homologue with a high threshold for noxious heat. *Nature* **398**, 436–441 (1999).
6. J. W. Leem, W. D. Willis, J. M. Chung, Cutaneous sensory receptors in the rat foot. *J. Neurophysiol.* **69**, 1684–1699 (1993).
7. R. H. LaMotte, J. G. Thalhammer, H. E. Torebjörk, C. J. Robinson, Peripheral neural mechanisms of cutaneous hyperalgesia following mild injury by heat. *J. Neurosci.* **2**, 765–781 (1982).
8. U. Park *et al.*, TRP vanilloid 2 knock-out mice are susceptible to perinatal lethality but display normal thermal and mechanical nociception. *J. Neurosci.* **31**, 11425–11436 (2011).
9. M. P. Neeper *et al.*, Activation properties of heterologously expressed mammalian TRPV2: Evidence for species dependence. *J. Biol. Chem.* **282**, 15894–15902 (2007).

10. A. Perálvarez-Marín, P. Doñate-Macian, R. Gaudet, What do we know about the transient receptor potential vanilloid 2 (TRPV2) ion channel? *FEBS J.* **280**, 5471–5487 (2013).
11. T. M. Link *et al*., TRPV2 has a pivotal role in macrophage particle binding and phagocytosis. *Nat. Immunol.* **11**, 232–239 (2010).
12. M. Kashio *et al*., Redox signal-mediated sensitization of transient receptor potential melastatin 2 (TRPM2) to temperature affects macrophage functions. *Proc. Natl. Acad. Sci. U.S.A.* **109**, 6745–6750 (2012).
13. C. H. Tan, P. A. McNaughton, The TRPM2 ion channel is required for sensitivity to warmth. *Nature* **536**, 460–463 (2016).
14. K. Song *et al*., The TRPM2 channel is a hypothalamic heat sensor that limits fever and can drive hypothermia. *Science* **353**, 1393–1398 (2016).
15. S. Yamamoto *et al*., TRPM2-mediated Ca2+ influx induces chemokine production in monocytes that aggravates inflammatory neutrophil infiltration. *Nat. Med.* **14**, 738–747 (2008).
16. A. Di, T. Kiya, H. Gong, X. Gao, A. B. Malik, Role of the phagosomal redox-sensitive TRP channel TRPM2 in regulating bactericidal activity of macrophages. *J. Cell Sci.* **130**, 735–744 (2017).
17. A. Hinman, H. H. Chuang, D. M. Bautista, D. Julius, TRP channel activation by reversible covalent modification. *Proc. Natl. Acad. Sci. U.S.A.* **103**, 19564–19568 (2006).
18. L. J. Macpherson *et al*., Noxious compounds activate TRPA1 ion channels through covalent modification of cysteines. *Nature* **445**, 541–545 (2007).
19. H. H. Chuang, S. Lin, Oxidative challenges sensitize the capsaicin receptor by covalent cysteine modification. *Proc. Natl. Acad. Sci. U.S.A.* **106**, 20097–20102 (2009).
20. A. Leffler, R. M. Linte, C. Nau, P. Reeh, A. Babes, A high-threshold heat-activated channel in cultured rat dorsal root ganglion neurons resembles TRPV2 and is blocked by gadolinium. *Eur. J. Neurosci.* **26**, 12–22 (2007).
21. B. Liu, F. Qin, Use dependence of heat sensitivity of vanilloid receptor TRPV2. *Biophys. J.* **110**, 1523–1537 (2016).
22. V. Juvin, A. Penna, J. Chemin, Y. L. Lin, F. A. Rassendren, Pharmacological characterization and molecular determinants of the activation of transient receptor potential V2 channel orthologs by 2-aminoethoxydiphenyl borate. *Mol. Pharmacol.* **72**, 1258–1268 (2007).
23. K. Susankova, K. Tousova, L. Vyklicky, J. Teisinger, V. Vlachova, Reducing and oxidizing agents sensitize heat-activated vanilloid receptor (TRPV1) current. *Mol. Pharmacol.* **70**, 383–394 (2006).
24. M. A. Ciorba, S. H. Heinemann, H. Weissbach, N. Brot, T. Hoshi, Modulation of potassium channel function by methionine oxidation and reduction. *Proc. Natl. Acad. Sci. U.S.A.* **94**, 9932–9937 (1997).
25. X. D. Tang *et al*., Oxidative regulation of large conductance calcium-activated potassium channels. *J. Gen. Physiol.* **117**, 253–274 (2001).
26. J. M. Huang, J. Tanguy, J. Z. Yeh, Removal of sodium inactivation and block of sodium channels by chloramine-T in crayfish and squid giant axons. *Biophys. J.* **52**, 155–163 (1987).
27. M. Kassmann *et al*., Oxidation of multiple methionine residues impairs rapid sodium channel inactivation. *Pflugers Arch.* **456**, 1085–1095 (2008).
28. M. Lévêque *et al*., Phagocytosis depends on TRPV2-mediated calcium influx and requires TRPV2 in lipids rafts: Alteration in macrophages from patients with cystic fibrosis. *Sci. Rep.* **8**, 4310 (2018).
29. N. W. Bellono, L. G. Kammel, A. L. Zimmerman, E. Oancea, UV light phototransduction activates transient receptor potential A1 ion channels in human melanocytes. *Proc. Natl. Acad. Sci. U.S.A.* **110**, 2383–2388 (2013).
30. A. Babes *et al*., Photosensitization in porphyrias and photodynamic therapy involves TRPA1 and TRPV1. *J. Neurosci.* **36**, 5264–5278 (2016).
31. K. Takeuchi, K. Yoshii, Effect of superoxide derived from lucifer yellow CH on voltage-gated currents of mouse taste bud cells. *Chem. Senses* **33**, 425–432 (2008).
32. D. A. Andersson *et al*., Streptozotocin stimulates the ion channel TRPA1 directly: Involvement of peroxynitrite. *J. Biol. Chem.* **290**, 15185–15196 (2015).
33. M. Entin-Meer *et al*., TRPV2 knockout mice demonstrate an improved cardiac performance following myocardial infarction due to attenuated activity of peri-infarct macrophages. *PLoS One* **12**, e0177132 (2017).
34. Y. Katanosaka *et al*., TRPV2 is critical for the maintenance of cardiac structure and function in mice. *Nat. Commun.* **5**, 3932 (2014).
35. W. Sun, K. Uchida, M. Tominaga, TRPV2 regulates BAT thermogenesis and differentiation. *Channels (Austin)* **11**, 94–96 (2017).
36. W. Sun *et al*., Lack of TRPV2 impairs thermogenesis in mouse brown adipose tissue. *EMBO Rep.* **17**, 383–399 (2016).
37. J. Vriens, T. Voets, Sensing the heat with TRPM3. *Pflugers Arch.* **470**, 799–807 (2016).
38. T. Voets, Quantifying and modeling the temperature-dependent gating of TRP channels. *Rev. Physiol. Biochem. Pharmacol.* **162**, 91–119 (2012).
39. N. Takahashi *et al*., TRPA1 underlies a sensing mechanism for O_2. *Nat. Chem. Biol.* **7**, 701–711 (2012).
40. K. W. Huynh *et al*., Structure of the full-length TRPV2 channel by cryo-EM. *Nat. Commun.* **7**, 11130 (2016).
41. L. Zubcevic *et al*., Cryo-electron microscopy structure of the TRPV2 ion channel. *Nat. Struct. Mol. Biol.* **23**, 180–186 (2016).
42. M. J. Caterina, Z. Pang, TRP channels in skin biology and pathophysiology. *Pharmaceuticals (Basel)* **9**, E77 (2016).
43. H. S. Park *et al*., Cutting edge: Direct interaction of TLR4 with NAD(P)H oxidase 4 isozyme is essential for lipopolysaccharide-induced production of reactive oxygen species and activation of NF-kappa B. *J. Immunol.* **173**, 3589–3593 (2004).
44. M. J. Eberhardt *et al*., Reactive metabolites of acetaminophen activate and sensitize the capsaicin receptor TRPV1. *Sci Rep* **7**, 12775 (2017).